Consideration of Impact Behaviour of Radioactive Packages onto Real Targets

K.Shirai, H.Akamatsu, C.Ito and H.Ryu

Central Research Institute of Electric Power Industry, Chiba, Japan
Maeda Corporation, Tokyo, Japan

INTRODUCTION

According to the IAEA Regulations for the Safe Transport of Radioactive Materials, a 9 m drop test is required for a type B packages as a test condition which simulates accidents in transport, e.g., fall, crash of the packages IAEA, 1985). The target provided for this drop test is an unyielding object surface; therefore, all kinetic energy of the dropping packages just before the impact is absorbed by the deformation of the packages. On the other hand, in the occurrence of real accidents, the object hardness needs to be considered. Since the packages can strike object surfaces such as concrete abutments, roadbeds, hard soil, and water, a part of the kinetic energy of the dropping packages just before the impact is absorbed by the deformation of the object surface. Consequently, it is expected that the hardness of the objects affects the impact response of the packages greatly. For example, the same impact force on the packages can be generated by a low-velocity impact on a hard object or a high-velocity impact on a soft object.
In this study, drop tests onto various object surfaces were performed using a 48Y-cylinder in order to clarify the relation between the object surface hardness and the associated impact response of the packages. Moreover, the Distinct Element Method (DEM) was applied to simulate the dynamic fracture impact behaviours of the real targets, and the effectivness of this method was investigated.

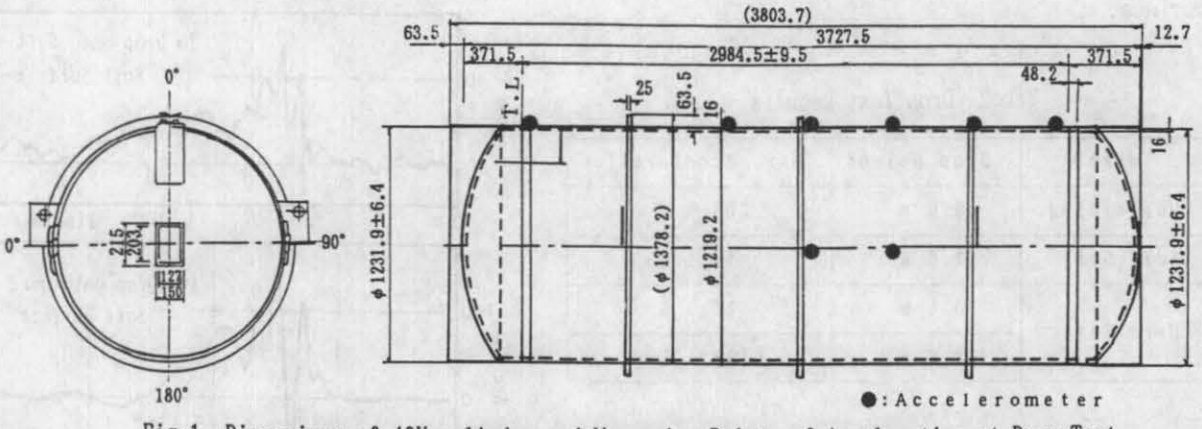

Fig. 1 Dimensions of 48Y-cylinder and Measuring Points of Acceleration at Drop Test

DROP TEST

Description of Test

Drop Tests using a 48Y-cylinder were performed at the Yokosuka Research Laboratory of CRIEPI (Kanagawa, Japan) considering target object hardness in real drop accidents. Dimensions of the 48Y-cylinder are shown in Fig. 1. Total weight was about 15,000 kg. Regarding natural uranium-hexaflouride, dummy granular steels equal to the total weight of the contents were used. As for the object target, the unyielding object surface described in the IAEA regulations for the Safe Transport of Radioactive Materials and the soft/hard soil object surface representing the hardness of earth surfaces was applied. A schematic view of drop test and test condition are shown in Fig. 2 and Tab. 1, respectively. Drop orientation was horizontal and a soft/hard soil object surface was made of sand which was charged and compacted in the steel enclosure. To estimate the impact force on the 48Y-cylinder during the drop tests, acclerations were measured at various points in the 48Y-cylinder, as shown in Fig. 1.

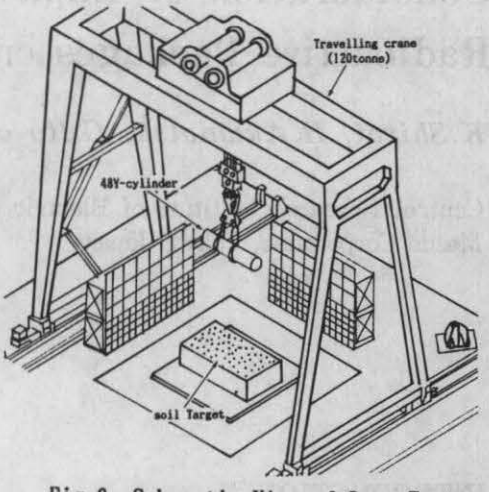

Fig. 2 Schematic View of Drop Test

Tab. 1 Drop Test Condition

Packaging	48Y-cylinder		
Weight	15,000kg		
Orientation	Horizontal		
Target	unyielding	soft soil	hard soil
Drop Height	9.0m	3.0m	0.6m, 14.0m

Drop Test Results

Measured time histories of the acclerometer at various points in the 48Y-cylinder are shown in Fig. 3. The high frequency components were removed from these time histories by a low pass filter (320Hz). The maximum acceleration values measured in various tests are summarized in Tab. 2. It was found that the maximum acceleration values occurring in drop tests onto a soil object surface were reduced considerably as compared with the value obtained in the drop test onto the unyielding object surface.

Tab. 2 Drop Test Results

Target	Drop Height	Max. Accelaration
Unyielding	9.0 m	203.6 G
Soft Soil	3.0 m	14.1 G
Hard Soil	0.6 m	12.3 G
	14.0 m	138.1 G

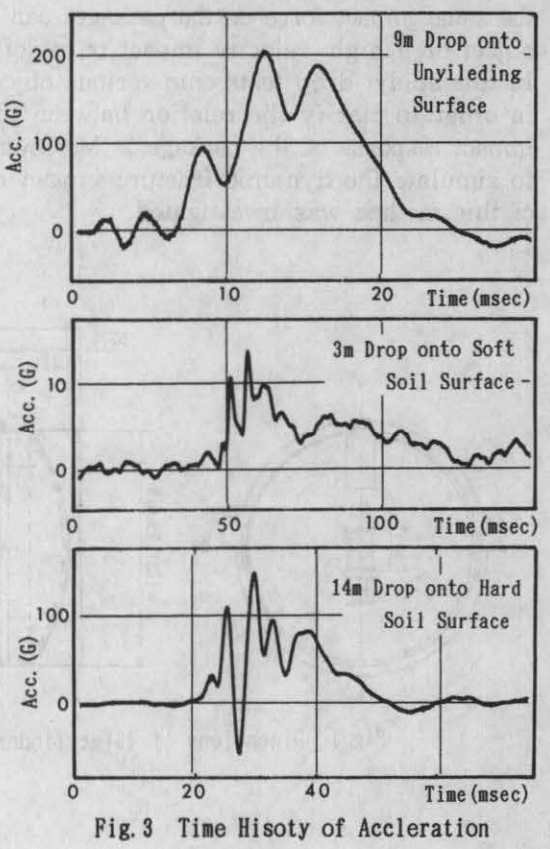

Fig. 3 Time Hisoty of Accleration

Drop Analysis using DEM

In order to clarify the drop impact characteristics of the 48Y-cylinder onto real targets, we applied DEM to drop analysis.

Theoretical Bases of DEM

DEM was introduced by Cundall P.A. (Cundall, 1971). DEM is based on the assumption that each element satisfies the equation of motion and the transmission of force between the elements following the law of action and reaction. In DEM analyis, a medium is treated as a rigid circular block assemblage. The motion of an individual block (Meguro et al. 1988) is determined by the magnitude and direction of the resultant out-of-balance moment and the force acting on it, and it is under the control of Newton's second law. The motion of a circular block having a mass m and a moment of inertia I is expressed as equation (1).

$$m\ddot{u} + c\dot{u} + F = 0$$
$$I\ddot{\theta} + c r^2 \dot{\theta} + M = 0 \quad \cdots\cdots \quad (1)$$

were F is the sum of all forces acting on the granular particle
M is the sum of all moments acting on it
c is the damping coefficient
u is the displacement vector and θ is the angular displacement

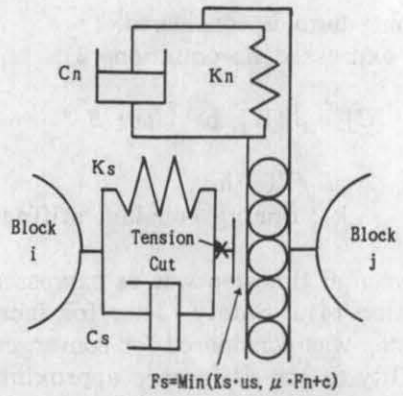

Fig. 5 Spring-Slider System at Contact Point

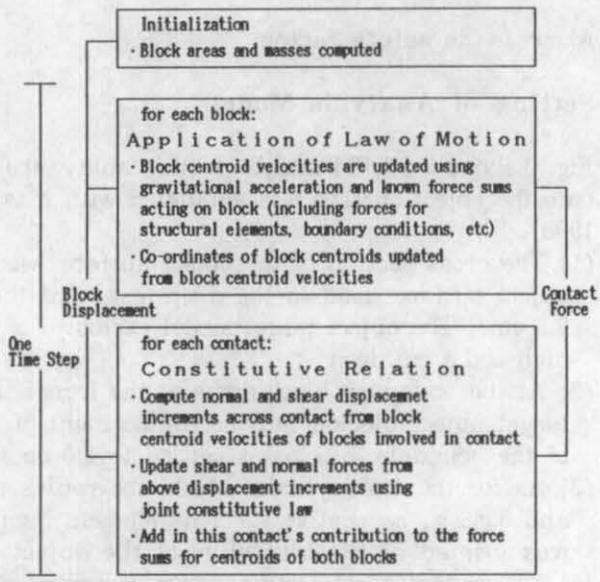

Fig. 4 Diagram Showing the Overall Calculation Flow of the DEM Code

The solutions to the equation of motion are obtained through a central difference scheme. Fig. 4, shows the diagram of the calculation flow. For the two adjacent blocks i (of a radius r_i) and j (of a radius r_j), the condition of the state of contact is expressed as equation (2).

$$r_i + r_j \leqq R_{ij} \quad \cdots\cdots \quad (2)$$

where R_{ij} is the relative displacement between two adjacent block centroids.
The deformability of the discontinuities or interfaces between blocks and the frictional characteristics are represented by spring-slider systems located at contact points between blocks as shown in Fig. 5, and the tension cut value is considered in the compressional forces. The acting force is divided into two components at the contacting point: a compressional force acting in the normal direction and a shear force acting in tangential direction. The acting force between blocks is calculated by the amount of penetration between two adjacent blocks which can be defined directly from block centroid translation and rotation. Shear forces are considered to be the frictional forces and limited by a Mohr-Coulomb friction law. As for damping, Reileigh daming is applied, and only stiffness

damping term is considered.
It is expressed as equation (3).

$$[C] = \beta [K],\ h = 2\omega \cdot \beta \quad \cdots\cdots \quad (3)$$

where $\omega = \sqrt{K / m}$

k : Spring constant stiffness

Incremental timestep was as expressed equation (4). Safety factor for incremental timestep was considered for convergence and stability of the difference approximation solution.

$$\Delta t = f_s \cdot 2\sqrt{m / K} \quad \cdots\cdots \quad (4)$$

where f_s is safety factor

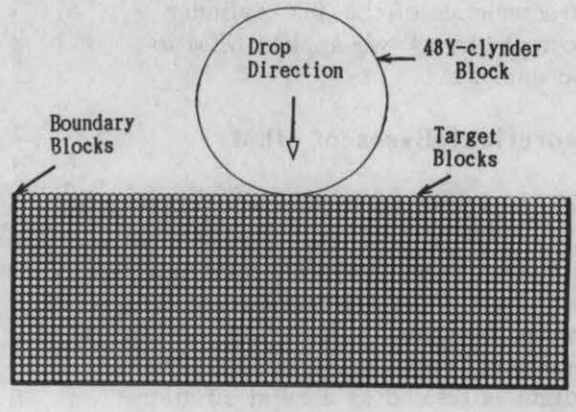

Fig. 6 DEM Model

Setting of Analysis Model

Fig. 6 shows the DEM model. In this study, the drop impact problem of the 48Y-cylinder onto the object surface was simulated with a two dimensional model as follows (Masuya et al. 1990).

(1) The cross section of the object surface was approximated by the dimensions of the soil object surface used in the drop test, and the radius of the target block was settled to 2.5 cm. The object target model exclusive of boundary blocks, was 350 cm wide, 120 cm high and 1 cm deep.
(2) At the boundary block domain, the force-displacement relation is the same as for target object blocks, but the diplacement of boundary blocks was set to zero. The radius of the boundary block was settled to 1.0 cm.
(3) As for the 48Y-cylinder block, the radius and mass of the block were settled to 62.56 cm and 3986 g, respectively. This element, ignoring the deformability of the 48y-cylinder, was located at the centerline of the object surface with an initial velocity.
(4) The contact normal stiffness Kn was represented by the Young modulus, and the contact shear stiffness Ks was settled to s · Kn obtained from multiplying Kn by reduction factor s. The analysis parameters are summarized as shown in Tab. 3 (Kiyama, 1983).
(5) For the relationship between block disposition and contact length, the square and hexagon type disposition were employed as shown in Fig. 7. The square type disposition (void ratio 0.273) was used for concrete and soft soil object targets, and the hexagon type disposition (void ratio 0.103) was used for hard soil and water object targets.

Tab. 3 Parameters for DEM Analysis

Target*	Density (g/cm^3)	Friction Angle	Stiffness** Kn(Mdyne/cm)	Damping** Cn(Mdyne·s/cm)	Cohesion (Mdyne)	Tension Cut (Mdyne)	Disposition
Concrete	2.50	37°	1.37×10^5	9.17×10^3	104.4	162.2	Square
Hard Soil	2.00	30°	7.35×10^2	6.01×10	0.0	0.0	Hexagon
Soft Soil	2.00	30°	7.35×10^2	6.01×10	0.0	0.0	Square
Water	1.10	0°	2.68×10^2	2.69×10	0.0	0.0	Hexagon

* : Target Block radius was settled to 2.5cm.
** : Ks and Cs were calculated from Kn/4 and Cn/4, respectively.

Analysis Results

The position of each block in the case of a 7 m drop analysis onto the hard soil and water object surface is shown in Fig. 8. When the 48Y-cylinder penetrates the object surface, a significant movement of blocks occurred around the 48Y-cylinder. Moreover, the penetration force of the 48Y-cylinder was transmitted widely in the horizontal direction, and the target blocks within a region near the ground surface around the boundary blocks were scattered. In Fig. 9, the test results and the analysis results were compared as to the acceleration time history in the case of the 14 m drop test onto hard soil and the 3 m drop test onto soft soil. The maximum acceleration and the frequency characteristics were in good agreement with the test results in both cases. Thus, it is confirmed that accuracy of the drop analysis onto real targets using DEM seems to be good enough to estimate the impact load occurring in the packages.

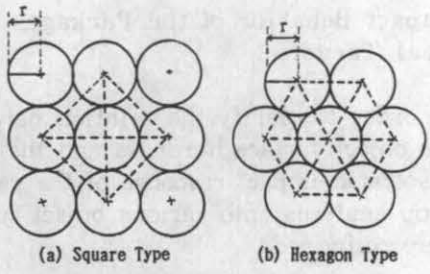

Fig. 7 Disposition of Block

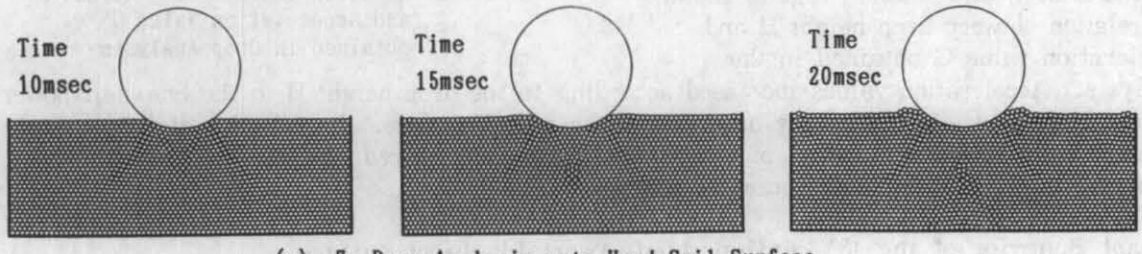

(a) 7m Drop Analysis onto Hard Soil Surface

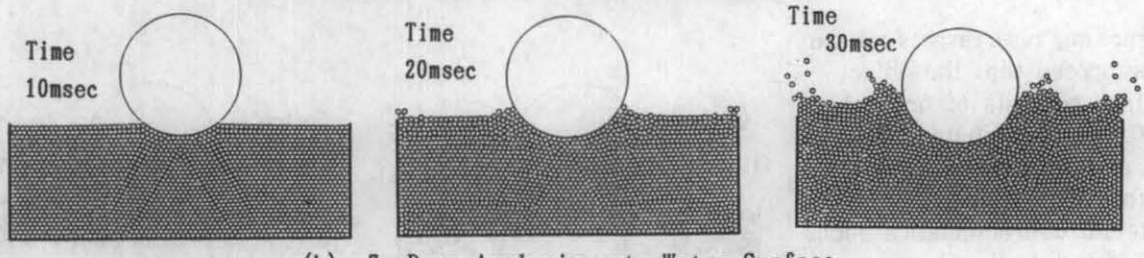

(b) 7m Drop Analysis onto Water Surface

Fig. 8 Penetration of the 48Y-cylinder into the Target Sarface

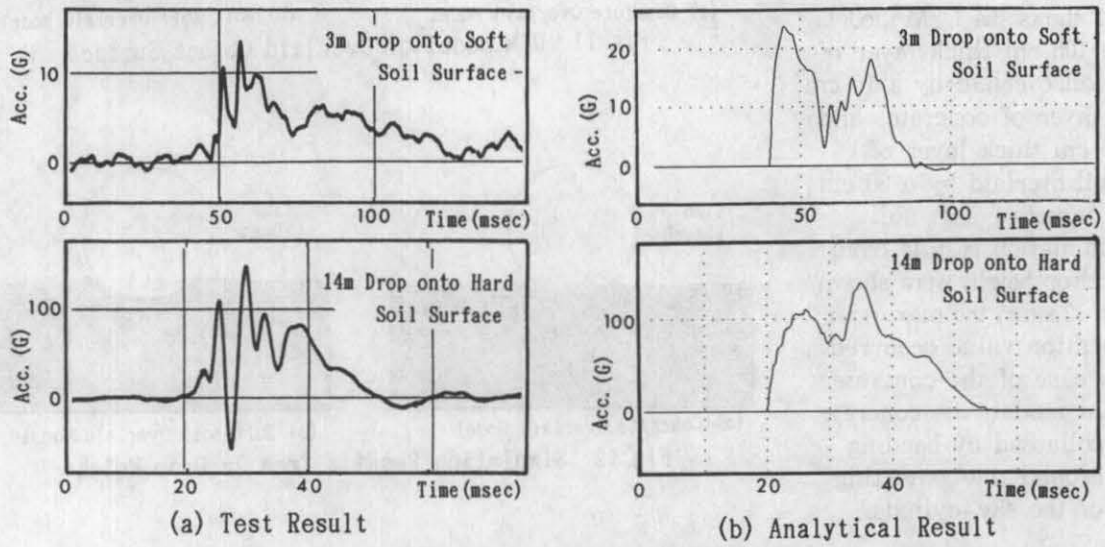

(a) Test Result

(b) Analytical Result

Fig. 9 Comparison between Test Results and Analytical Results

Impact Behavior of the Packages onto Real Targets

In order to clarify the relation between the object surface hardness and the associated impact response of the packages, drop analyses onto various object surfaces were performed.

Impact Behavior of the 48Y-cylinder onto an uniformly distributed surface

Drop analysis onto an uniform layer surface target was performed using the DEM model as shown in Fig. 6. The target provided for these drop analyses were concrete, hard/soft soil, and water. Fig. 10 shows the relation between drop height H and acceleration value G obtained in the analysis. Acceleration values increased according to the drop height H to the one-half power, and were greatly affected by the hardness of the object surface. In the case of the concrete surface, since the deformability of the 48Y-cylinder was ignored, the acceleration value occurring in the 48Y-cylinder increased extremely.

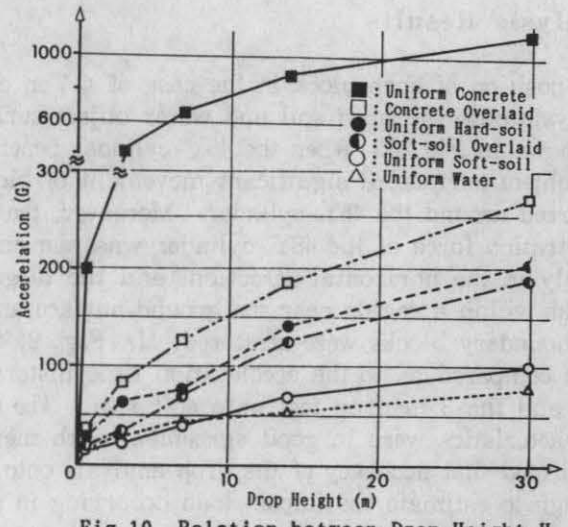

Fig. 10 Relation between Drop Height H and Accerelation Value G obtained in Drop Analysis

Impact Behavior of the 48Y-cylinder onto overlaid object surface

Regarding real targets, it can be supposed that the object surface consists of not only uniformly distributed material, but also an overlaid object surface which has different material characteristics such as a paved road. So, drop analysis onto an overlaid object surface was performed. Fig. 11 shows the DEM models of the 105 cm thick layer of hard soil overlaid by a 15 cm thick layer of concrete, and the 90 cm thick layer of hardsoil overlaid by a 30 cm thick layer of soft soil. The simulation results from a 7 m drop height were shown in Fig. 12 when the maximum acceleration value occurred. In the case of the concrete overlaid model, the concrete layer collapsed by bending force around the contacting point of the 48y-cylinder block.

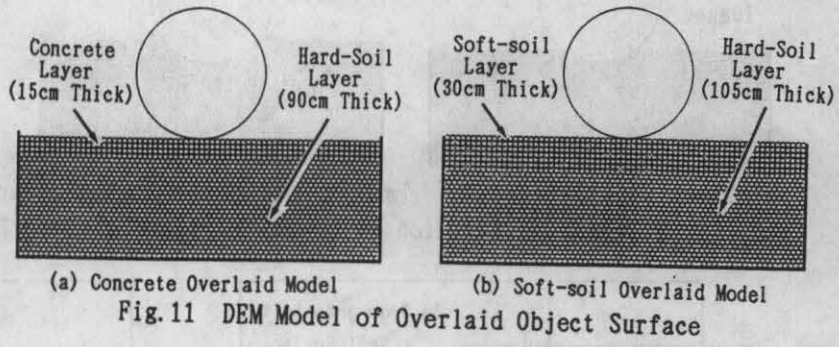

Fig. 11 DEM Model of Overlaid Object Surface

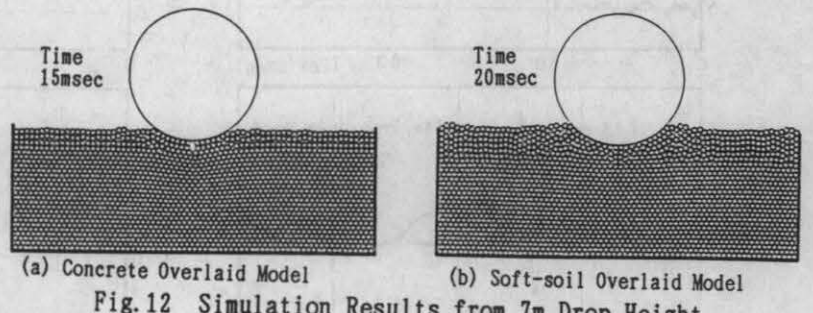

Fig. 12 Simulation Results from 7m Drop Height

Deformability of the 48Y-cylinder

In the previous analysis, the deformability of 48Y-cylinder was ignored. So, in this paragraph, the deformability of the 48Y-cylinder was discussed. The load-deflection characteristic of the 48Y-cylinder was investigated by static structural analysis using NIKE-3D. Fig. 13 shows a finite element model and material property. The 48Y-cylinder body was modeled using a four node shell element, and in consideration of the contents in the cylinder, an additional mode force equal to the total weight of the cylinder was applied.
The relation between the static forced acceleration and the equivalent drop height calculated from energy absorption of the cylinder was shown in Fig. 14. The static acceleration value was 135 G for a 9 m equivalent drop height. Since the maximum dynamic accerelation that occurred in the drop tests was 200G, the dynamic magnification factor for acceleration was about 1.5.

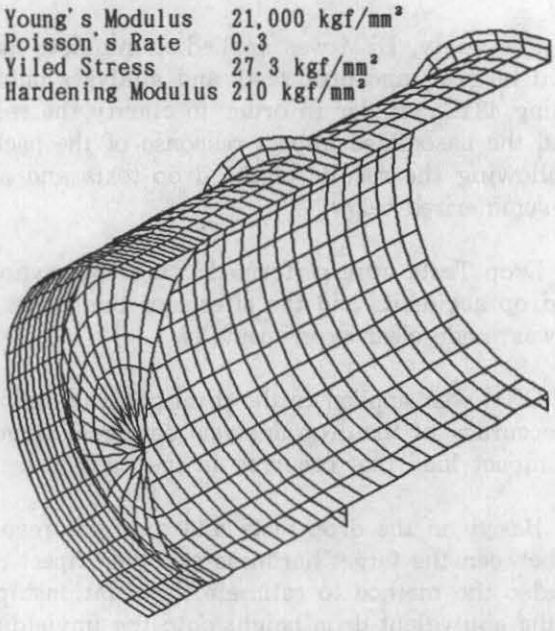

Fig. 13 Finite Element Model and Material Property

Relation between the target hardness and the impact response of 48Y-cylinder

Fig. 15 shows the relation between the object surface hardness and the associated impact response of the 48Y-cylinder. A full line curve with symbol denotes the relation in the case of the drop impact onto the unyielding surface which was calculated from multiplying the acceleration-height curve obtained from static structural analysis by the dynamic magnification factor. It is assumed that the drop impact force onto the 120 cm thick uniform concrete surface is nearly the same as the case of the unyielding object surface. It can be considered that the effect of the drop impact response of the packages on the hardness of the object surface will be estimated through this figure with the proposed analysis method. For example, the same impact force on the packages from 9 m drop height onto the unyielding surface can be generated by a drop impact from 17 m height onto concrete overlaid surface or a drop impact from 29 m height onto hard soil surface.

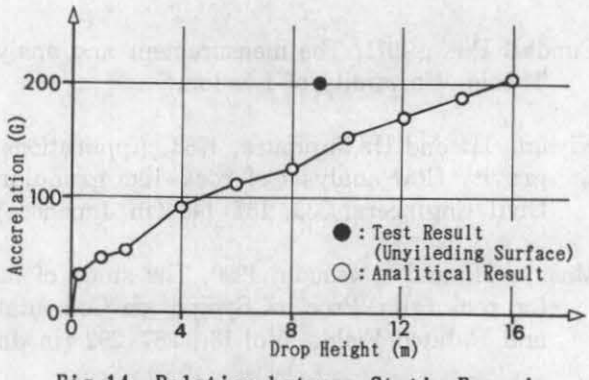

Fig. 14 Relation between Static Forced Accerelation Value G and Equivalent Drop Height H

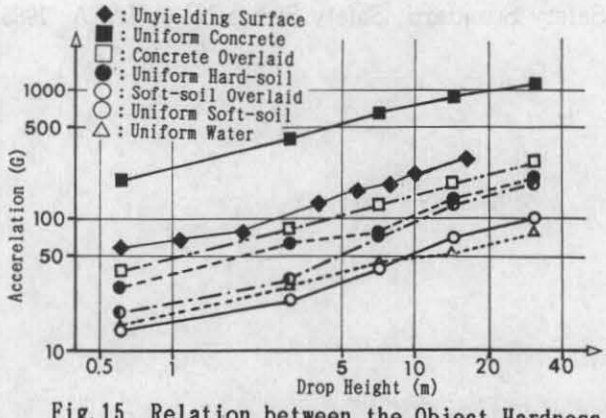

Fig. 15 Relation between the Object Hardness and the Associated Impact Response of the 48Y-cylinder

CONCLUSION

In this study, DEM was applied to simulate the dynamic fracture impact behaviours of the real targets, and drop tests and analyses onto various object surfaces were performed using 48Y-cylinder in order to clarify the relation between the object surface hardness and the associated impact response of the packages.
Following the results of the drop tests and analyses, the outline of contents and results is summarized below.

1) Drop Tests were performed using 48Y-cylinder considering target object hardness in real drop accidents and the effects of the target object hardness on the drop impact response was made clear experimentally.

2) DEM was applied to the drop analysis onto real targets and it is confirmed that the accuracy of the drop analysis onto real targets using DEM is good enough to estimate the impact load that occurred in the packages.

3) Based on the drop tests and analysis results onto various object surfaces, the relation between the target hardness and the impact response of 48Y-cylinder was made clear, and also the method to estimate the relationship between the drop height for real targets and the equivalent drop height onto the unyielding surface was proposed.

REFERENCES

Cundall P.A., 1971, The measurement and analysis of accelerations in rock slopes, Ph. D. Thesis, University of London.

Kiyama H. and H. Fujimura, 1983, Applications of cundall's discrete block method to gravity flow analysis of rock-like granular materials, Proc. Japan Society of Civil Engineers, 333, 137-146 (in Japanese).

Masuya H. and S.Masuda, 1990, The study of the impact characteristic of the cushion for rock falls, Proc. of Sympo. on Computational Methods in Structural Engineering and Related Fields, Vol.16., 287-292 (in Japanese).

Meguro K. and H.Hakuno, 1988, Fracture Analysis of Concrete Structures by Granular Assembly Simulation, Bull. Earthq. Res. Inst., Univ. Tokyo, Vol.63, 409-468 (in Japanese)

Safety Standard, Safety Series No.6, IAEA, 1985.

REGULATIONS, SYSTEM ANALYSIS,
ENVIRONMENTAL IMPACTS, AND RISK ASSESSMENT

Session 30:

EMERGENCY RESPONSE

Chairman : M. L. Miller
Co-Chairman : H. Ohnuma
Coordinator : K. Jikuhara